

Histone deacetylase inhibitor- and PMA-induced upregulation of PMCA4b enhances Ca²⁺ clearance from MCF-7 breast cancer cells

Karolina Varga^a, Katalin Pászty^b, Rita Padányi^c, Luca Hegedűs^a, Jean-Philippe Brouland^d, Béla Papp^e, and Agnes Enyedi^{a,c,*}

^a Institute of Molecular Pharmacology, Research Centre for Natural Sciences, Hungarian Academy of Sciences, Budapest, Hungary

^b Molecular Biophysics Research Group of the Hungarian Academy of Sciences and Department of Biophysics, Semmelweis University, Budapest, Hungary

^c Department of Molecular Cell Biology, Hungarian National Blood Transfusion Service, Budapest, Hungary

^d Service d'Anatomie et Cytologie Pathologiques, Hôpital Lariboisière, Paris, France

^e Institut National de la Santé et de la Recherche Médicale, U978 and Université Paris-13, PRES Sorbonne Paris-Cité, Bobigny, France

* To whom correspondence should be addressed: Agnes Enyedi, Institute of Molecular Pharmacology, Research Centre for Natural Sciences, HAS and Department of Molecular Cell Biology, Hungarian National Blood Transfusion Service. Dioszegi ut 64, H-1113 Budapest, Hungary. Tel/Fax: +36 1 372 4353. E-mail: enyedi@biomembrane.hu

Abstract

The expression of the plasma membrane Ca^{2+} ATPase (PMCA) isoforms is altered in several types of cancer cells suggesting that they are involved in cancer progression. In this study we induced differentiation of MCF-7 breast cancer cells by histone deacetylase inhibitors (HDACis) such as short chain fatty acids (SCFAs) or suberoylanilide hydroxamic acid (SAHA), and by phorbol 12-myristate 13-acetate (PMA) and found strong upregulation of PMCA4b protein expression in response to these treatments. Furthermore, combination of HDACis with PMA augmented cell differentiation and further enhanced PMCA4b expression both at mRNA and protein levels. Immunocytochemical analysis revealed that the upregulated protein was located mostly in the plasma membrane. To examine the functional consequences of elevated PMCA4b expression, the characteristics of intracellular Ca^{2+} signals were investigated before and after differentiation inducing treatments, and also in cells overexpressing PMCA4b. The increased PMCA4b expression – either by treatment or overexpression – led to enhanced Ca^{2+} clearance from the stimulated cells. We found pronounced PMCA4 protein expression in normal breast tissue samples highlighting the importance of this pump for the maintenance of mammary epithelial Ca^{2+} homeostasis. These results suggest that modulation of Ca^{2+} signaling by enhanced PMCA4b expression may contribute to normal development of breast epithelium and may be lost in cancer.

1. Introduction

Plasma membrane Ca^{2+} ATPases (PMCA) play an important role in maintaining intracellular Ca^{2+} homeostasis. These pumps are responsible for the expulsion of increased intracellular Ca^{2+} into the extracellular space [1, 2]. The four major isoforms (PMCA1-4) are encoded by separate genes and, as a consequence of alternative RNA splicing, more than 20 variants exist. The different PMCA variants show tissue- and cell-specific expression patterns and regulate in different ways the maintenance of the normally low cytosolic Ca^{2+} concentration [3]. Therefore, the expression, localization and activity of the different PMCA isoforms need to be precisely controlled to fulfill properly their role [2, 4].

Recently several articles have been published that suggest a potential role of intracellular Ca^{2+} homeostasis remodeling in cancer progression [5-7]. However, only a few of them focus on the PMCA [8, 9], and these generally report decreased expression of certain PMCA isoforms while increased expression of others in different cancer cells or tissue samples. PMCA1b and 4b expression was lower in SV40 transformed human skin and lung fibroblasts than in the corresponding parental cell lines [10]. mRNA expression studies on breast cancer cell lines showed upregulated PMCA1 and 2 and downregulated PMCA4 expression in some breast cancer cells compared to non-tumorigenic cell lines [11, 12]. PMCA1 was found to be epigenetically inactivated in oral squamous cell carcinoma-derived cell lines, and PMCA1 protein was frequently downregulated in primary oral squamous cell carcinoma and oral premalignant lesion tissue samples [13]. Furthermore, downregulation of PMCA4 expression in colon carcinoma has been reported while a comparatively high level of PMCA4 was detected in normal colon tissue [14, 15].

Several lines of evidence have suggested that during differentiation of the tumor cells some PMCA isoforms are upregulated. Expression of PMCA 2, 3 and 4 isoforms were

enhanced during differentiation of the neuroblastoma cell line IMR-32, and this resulted in increased Ca^{2+} efflux [16]. Short chain fatty acids (SCFAs) are histone deacetylase inhibitors that can inhibit proliferation of tumor cells, induce differentiation and apoptosis [17-24]. Therefore, several histone deacetylase inhibitors like suberoylanilide hydroxamic acid (SAHA, Vorinostat) or valproate (VPA) are used in clinical trials as anticancer drugs [17]. Recent experiments demonstrated that SCFA-triggered differentiation upregulated PMCA4b expression in a variety of gastric and colon cancer cells [25, 26]. The protein kinase C activator phorbol 12-myristate 13-acetate (PMA) has also been shown to cause differentiation in MCF-7 cells [20-22], and as suggested by others it can induce PMCA mRNA and protein expression in vascular endothelial cells [27].

In this study we examined the effect of HDACis and PMA on the expression of PMCA in the MCF-7 cell line which is a commonly used breast cancer model for studying the mechanisms of tumor progression. We found marked PMCA4b upregulation during HDACi-induced differentiation that was further enhanced by PMA, while there were no remarkable changes in the expression levels of the other PMCA isoforms. The increased PMCA4b expression led to enhanced Ca^{2+} clearance from the cells stimulated with various calcium mobilizing agents. PMCA4 protein was also found in normal breast epithelial cells, suggesting that this protein plays a role in the regulation of Ca^{2+} homeostasis of the mammary epithelium.

2. Materials and methods

2.1. Cell culture

The MCF-7 breast cancer cell line (ATCC HTB-22) was obtained from The American Type Culture Collection, and was cultured in DMEM supplemented with 10% FBS, 100 U/ml

penicillin, 100 µg/ml streptomycin and 2 mM glutamine at 37°C and 5% CO₂ in a humidified atmosphere.

2.2. *Treatments of MCF-7 cells*

Short chain fatty acids (butyric acid, 4-phenylbutyric acid and valeric acid; purchased from Sigma-Aldrich) were dissolved at 300 mM concentration in equimolar sterile sodium bicarbonate solution then membrane filtered using a 0.2 µm filter and stored at -20°C. Valproic acid sodium salt (Sigma-Aldrich) was dissolved at 200 mM concentration in sterile distilled water, membrane filtered and stored at -20°C. Phorbol 12-myristate 13-acetate (PMA; Sigma-Aldrich), suberoylanilide hydroxamic acid (SAHA; Sigma-Aldrich) and GF 109203X hydrochloride (Sigma-Aldrich) stock solutions were made in DMSO and stored at -20°C. Exponentially growing cells were seeded at $1.5-2 \times 10^5$ cells/well in 6-well plates for Western blot and real time PCR analysis, at $8-9 \times 10^4$ cells/well in 24-well plates for analysis of cell proliferation and Oil Red O staining, at $3-4 \times 10^5$ cells per 6 cm diameter Petri dishes for immunoprecipitation and at $0.8-1 \times 10^5$ cells/well in Imaging Chamber CG 8 Well (PAA) for immunostaining and Ca²⁺ signal measurements. When cultures reached 80% confluency, medium was replaced by fresh DMEM and differentiation inducing drugs were added from concentrated stock solutions. During SAHA treatment the medium was replaced daily. The final DMSO concentration did not exceed 0.01% in all experiments, DMSO vehicle was included in controls and did not interfere with the experiments.

2.3. *Transfection*

Transient transfection with the mCherry-PMCA4x/b construct [28] was carried out using FuGENE HD Transfection Reagent (Roche Applied Science) according to the manufacturer's protocol.

2.4. *Generation of the stable GCaMP2-MCF-7 cell line*

To establish an MCF-7 cell line stably expressing the genetically encoded Ca^{2+} sensor GCaMP2, we used the Sleeping Beauty transposon system [29, 30]. Cells were cotransfected with the SB100 \times transposase plasmid and the SB-CAG-GCaMP2-CAG-Puro transposon construct [31] that contains a puromycin resistance gene, at a 1:10 ratio using FuGENE HD Transfection Reagent (Roche Applied Science). Two days post-transfection, culture medium was replaced by fresh medium containing 1 $\mu\text{g}/\text{ml}$ puromycin dihydrochloride (Santa Cruz Biotechnology) and selection was continued until all of the non-transfected cells died. During the selection period cells were monitored for GFP fluorescence using a fluorescent microscope, and medium was replaced by freshly made selective medium in every two days. The resulting polyclonal GCaMP2-MCF-7 cell line was used for Ca^{2+} signal measurements.

2.5. *Cell proliferation*

To examine cell proliferation, equal numbers of cells were treated with the indicated differentiating compounds for 4 days. After treatments, cells were washed twice with PBS, trypsinized and live cells were counted using an automated cell counter (Bio-Rad). Viability was assessed by the trypan blue exclusion method. Untreated control cells were counted before, and 4 days after treatments, as indicated.

2.6. *Oil Red O staining*

Cells were treated with the indicated differentiating agents for 4 days, then were washed twice with PBS and fixed with 4% paraformaldehyde in PBS for 15 min at 37°C. After washing two times with distilled water, cells were incubated with 60% isopropanol for 2 min, and then stained with Oil Red O (Sigma-Aldrich) dissolved at 1.8 mg/ml in 60% isopropanol,

for 10 min. Phase contrast and fluorescent images were captured with an Olympus CKX41 microscope using a 40× objective. Cell number and total area of lipid droplets per image were determined using the ImageJ software v1.42q.

2.7. Western blot analysis

Total protein from treated cells was precipitated by the addition of 6% TCA and was analyzed by Western blot as described previously [32]. Equal amounts of protein were loaded on 7.5% acrylamide gels, electrophoresed, electroblotted onto PVDF membranes (Bio-Rad) and immunostained. The following primary antibodies were used: mouse monoclonal anti-*pan* PMCA (5F10; dilution 1:5000), rabbit polyclonal anti-PMCA1 (NR1; dilution 1:500), rabbit polyclonal anti-PMCA2 (NR2; dilution 1:500), rabbit polyclonal anti-PMCA3 (NR3; dilution 1:500) and mouse monoclonal anti-PMCA4b (JA3; dilution 1:1000) described in [33, 34], rabbit polyclonal anti-PMCA1 (Affinity BioReagents, PA1-914; dilution 1:1000), mouse monoclonal anti-SERCA2 antibody (IID8; dilution 1:2500) obtained from Sigma-Aldrich (S1439), mouse monoclonal anti-SERCA3 (PL/IM430; dilution 1:200) described in [25] and mouse monoclonal anti-Na,K-ATPase (dilution 1:2000) from Enzo Life Sciences (BML-SA247). Subsequently, HRP-conjugated anti-mouse or anti-rabbit secondary antibodies (Jackson ImmunoResearch) were applied and detected by Pierce ECL Western Blotting Substrate (Thermo Scientific) and luminography. The ImageJ software v1.42q was used for densitometric analysis.

2.8. Immunoprecipitation

Cells were treated with 2 mM valerate in the presence or absence of 10 nM PMA for 4 days. PMCA proteins from whole cell lysates were enriched by immunoprecipitation with the 5F10 anti-*pan* PMCA antibody using the Pierce Co-Immunoprecipitation Kit (Thermo

Scientific). The experimental procedure was done according to the manufacturer's instructions except that the electrophoresis sample buffer contained 0.1 M dithiothreitol, 0.8 M urea and 5 mM EDTA-Na pH 6.8, and heating of the samples was omitted.

2.9. Real-time quantitative PCR

Cells were treated with 2 mM valerate in the presence or absence of 10 nM PMA for 4 days, and then total RNA was isolated with the peqGOLD TriFast reagent (Peqlab Biotechnologie) and subsequently reverse transcribed using the Reverse Transcription System (Promega) according to the instructions of the suppliers. Amplification of cDNA was performed using StepOnePlus Real-Time PCR System (Applied Biosystems) with TaqMan Gene Expression Master Mix and the following TaqMan Gene Expression Assays: Hs00155949_m1 for PMCA1, Hs01090453_m1 for PMCA2 and Hs00608066_m1 for PMCA4 (Applied Biosystems). Reactions were run under standard cycling conditions according to the supplier's recommendations. Quantitation of PMCA mRNA levels was done by StepOne software v2.1 (Applied Biosystems) according to the comparative C_T method, normalizing to RPLP0 (Hs99999902_m1) and POLR2A (Hs00172187_m1) endogenous controls.

2.10. Immunocytochemistry

After treatment with 2 mM valerate \pm 10 nM PMA for 4 days cells were washed twice with 37°C HBSS and fixed with 4% paraformaldehyde for 15 min at 37°C. After five washes with PBS, cells were permeabilized with ice cold methanol for 5 min and washed five times again with PBS. Subsequently, cells were incubated in blocking buffer (PBS containing 2 mg/ml bovine serum albumin, 1% fish gelatin, 0.1% Triton-X 100, 5% goat serum) for 1 h at RT and then immunostained with a mouse monoclonal anti-PMCA4b antibody (JA3; dilution

1:100) or a mouse monoclonal anti-PMCA4 antibody (JA9; dilution 1:100) [33] and with a chicken polyclonal anti-Na,K-ATPase antibody (Abcam, ab353; dilution 1:500) for 1 h at RT. After three washes with PBS, cells were incubated with Alexa Fluor anti-mouse and anti-chicken secondary antibodies (Invitrogen) for 1 h at RT and imaged with an Olympus IX-81 confocal laser scanning microscope and Fluoview FV500 software v4.1 using an Olympus PLAPO 60× (1.4) oil immersion objective. All images were taken with the same microscope settings.

2.11. Ca²⁺ signal measurements

GCaMP2-MCF-7 cells were treated with 2 mM valerate ± 10 nM PMA for 3 days, then the medium was replaced by fresh DMEM and cells were incubated in the absence of differentiating compounds for an additional day. For comparison, untreated GCaMP2-MCF-7 cells were transiently transfected with the mCherry-PMCA4x/b construct 2 days before Ca²⁺ signal measurements. Prior to the experiments cells were incubated for two hours in phenol red-free DMEM containing 10 mM HEPES pH 7.4 and 10% FBS. To measure store-operated Ca²⁺ entry, medium was replaced by nominally Ca²⁺ free HBSS supplemented with 0.9 mM MgCl₂, 100 μM EGTA, 100 μM CaCl₂ and 20 mM HEPES pH 7.4. Intracellular stores were depleted with 2 μM thapsigargin and subsequently with 100 μM ATP. After 5 min the external Ca²⁺ was restored to 2 mM by the addition of CaCl₂ and Ca²⁺ influx through store-operated Ca²⁺ channels was followed for 10 min. When Ca²⁺ signals were evoked by A23187, first the medium was replaced by HBSS supplemented with 0.9 mM MgCl₂, 2 mM CaCl₂ and 20 mM HEPES pH 7.4, and then Ca²⁺ influx was triggered by the addition of 2 μM A23187. Images were taken with an Olympus IX-81 confocal laser scanning microscope and Fluoview FV500 software v4.1 using an Olympus PLAPO 60× (1.4) oil immersion objective. For GCaMP2 imaging cells were excited at 488 nm and emission was collected between 505 and

535 nm. mCherry-PMCA4x/b was illuminated at 543 nm and emission above 560 nm was recorded. Images were acquired every 0.3 s, z-resolution was 1 μm . Time lapse sequences were recorded with Fluoview Tiempo time course software v4.3 at RT. The relative fluorescence intensities were calculated as F/F_0 (where F_0 was the average initial fluorescence) and data were analyzed with the Prism 4 software v4.01 (GraphPad Software).

2.12. Immunohistochemistry

Immunohistochemical staining for PMCA4 was performed with the JA9 mouse IgG1 monoclonal antibody (Sigma-Aldrich, P1494) on 5 μm thick deparaffinized formalin-fixed sections using an indirect avidin-biotin-peroxydase method and 3,3'-diaminobenzidine as chromogene. Immunostaining was performed on a Benchmark automatic immunostainer (Ventana Medical Systems), and inhibition of endogeneous peroxidase activity, biotin block and signal amplification were performed according to the protocol of the manufacturer. Antigen retrieval of deparaffinized sections by a *tris*-(hydroxymethyl)-aminomethane-based antigen retrieval reagent (Ventana CC1 cell conditioning solution) was done at 95-100°C for 30 min, and slides were incubated with the anti-PMCA4 antibody in Emerald Antibody Diluent (Cell Marque) at 3 $\mu\text{g}/\text{ml}$ for 30 min at 37°C. Staining was revealed using the Ventana I-View Biotin-Ig-streptavidin-horseradish peroxydase system with copper enhancement, according to the instructions of the manufacturer, and slides were counterstained with hematoxylin. In control experiments slides were stained with 3 $\mu\text{g}/\text{ml}$ of an irrelevant IgG1 monoclonal antibody at identical conditions, and this gave no staining.

2.13. Statistical analysis

Data were analyzed with Prism 4 software v4.01 (GraphPad Software) and are expressed as means \pm SD, except for the Ca^{2+} signal measurements where they are means \pm 95% CI.

Statistical significance was calculated by t-test, *** means $P < 0.001$, ** means $P < 0.01$, * means $P < 0.05$, n.s. means not significant.

3. Results

3.1. SCFAs and PMA enhanced the expression of PMCA4b in MCF-7 cells

SCFAs such as butyrate and its aryl-substituted analog phenylbutyrate are known differentiating agents in several experimental systems [20-24]. Moreover, they have been shown to enhance PMCA4b expression in colon cancer cells [25, 26]. In addition PMA has been suggested to induce differentiation of MCF-7 cells [20-22]. Therefore, we examined the effects of these differentiation inducing compounds on PMCA expression in MCF-7 cells [35]. After treating cells with butyrate, phenylbutyrate, valerate (SCFAs) or with PMA, the expression of PMCA isoforms was determined by Western blot analysis. Fig. 1A-D shows changes of PMCA protein levels at increasing concentrations of SCFAs and PMA. The 5F10 anti-*pan* PMCA antibody recognized two bands of which the upper band was also selectively detected by the anti-PMCA1 antibody while the lower band by the PMCA4b specific antibody JA3. PMCA1 was the main PMCA isoform in untreated MCF-7 cells but the expression pattern changed rather dramatically after treatments. Both SCFAs and PMA induced marked upregulation of PMCA4b expression without having much effect on the expression of the PMCA1 isoform. The level of Na,K-ATPase expression remained constant during the treatments and served as a control in further experiments. The increase of PMCA4b expression was maximal at 3-5 mM of the SCFA compounds used, and at 10 nM of PMA. Fig. 1E represents a time course of the treatments with the maximally effective SCFA and PMA concentrations (5 mM of butyrate, phenylbutyrate (PB) and valerate or 10 nM of PMA, as indicated). Increased PMCA4b expression could be detected as early as days 1 or 2 and the

protein expression reached a plateau-phase around the 4th day of treatment. The relative amount of PMCA4b (stained with antibody JA3, Fig. 1F) and total PMCA (*i.e.* PMCA1 and PMCA4 together stained with antibody 5F10, Fig. 1G) expressions were further assessed by semi-quantitative densitometric analysis of the Western blots. The level of PMCA4b protein was greatly enhanced (50-90 fold) during the treatments that resulted in a substantial increase (6-10 fold) of the overall PMCA protein expression.

3.2. *Effects of SCFAs and PMA on cellular proliferation and differentiation*

It is widely accepted that SCFAs inhibit cell proliferation and at higher concentrations induce apoptosis in various cancer cells [36-41] whereas, the effect of PMA on cell survival and proliferation appears to be more diverse; it depends on the contributing PKC isoform, the activity of interacting signaling pathways and the duration of treatment [21, 42-46]. Here we examined the proliferation rate of cells during a prolonged treatment (4 days) with SCFAs or PMA. Equal numbers of cells were treated with the appropriate compound and viable cells were counted using the trypan blue exclusion method. Fig. 2A shows that all SCFAs inhibited cell proliferation, and at higher concentrations (5 mM) significantly reduced the number of viable cells. A time course of the viability assay (Fig. 2B) shows that at a lower concentration of valerate (2 mM) growth inhibition was less pronounced and significant cell death could be detected only after longer incubation times. Therefore, in further experiments we treated cells with valerate instead of butyrate or phenylbutyrate because it resulted in more viable cells as it was shown previously [23, 24]. The proliferation of PMA treated cells was also diminished, however, no significant decrease of viability was observed during the 4 day treatment suggesting that in accordance with previous reports, PMA inhibited growth but did not cause significant cell death [44].

Differentiation results in the intracellular accumulation of Oil Red O positive lipid droplets which is a widely used phenotypic marker of differentiation in breast cancer cells [20, 22, 47]. Therefore, we used the Oil Red O staining procedure to verify the differentiation status of MCF-7 cells after exposure to SCFAs or PMA (Fig. 2C-E). Areas of lipid droplets per cells were determined using the ImageJ software (Fig. 2C,D). All treatments resulted in a great increase in the population of Oil Red O positive cells so that the area of lipid droplets per cell increased 9-15 fold in SCFA-treated cells compared to control. Previous studies showed that SCFA and PMA treatments acted synergistically in colon cancer [48] and intestinal epithelial cells [49], therefore, we tested the differentiation status of MCF-7 cells treated with SCFAs in combination with PMA. We found that PMA greatly potentiated the differentiation process induced by valerate (Fig. 2C-E) and maximal induction could be reached between day 2-3 (Fig. 2D).

3.3. Combined treatment by valerate and PMA further increased PMCA4b upregulation in MCF-7 cells

Our experiments showed that PMA potentiated SCFA-induced differentiation of MCF-7 cells; therefore, we tested how the combination of these treatments influenced PMCA expression. In these experiments we used valerate together with PMA and followed PMCA expression for up to 3 days. Fig. 3A-D demonstrates that the combined treatment highly augmented the upregulation of PMCA4b protein expression. A comparison of the time curves in Fig. 3D and Fig. 2D shows that both PMCA4b expression and cell differentiation reached their maximum level between day 2-3 suggesting correlation between these processes.

Other key factors of cellular Ca^{2+} homeostasis are the sarco/endoplasmic reticulum Ca^{2+} ATPases (SERCAs). Therefore, we examined changes in the expression level of the SERCA-type Ca^{2+} pumps in valerate \pm PMA-treated MCF-7 cells (Fig. 3A). A significant increase of

SERCA2 expression was observed when cells were treated with PMA alone, while SERCA3 levels increased in valerate-treated cells. These results are in agreement with earlier data showing reduced SERCA3 expression during breast epithelial tumorigenesis [50] and upregulated SERCA3 expression by SCFAs in several lung and colon cancer cell lines [51, 52].

To further characterize the PMCA expression pattern in MCF-7 cells PMCA proteins were specifically enriched by immunoprecipitation with the 5F10 anti-pan PMCA antibody, and samples were tested for the expression of all PMCA isoforms using isoform specific antibodies (Fig. 3E). The results of these experiments further support our data shown in Fig. 1A-D that PMCA1 was the major isoform in untreated MCF-7 cells, and that its expression did not increase after the treatments. On the other hand, while the expression of PMCA4b was relatively low in control cells, it was highly upregulated upon treatments. In contrast to previous findings [53], we could not detect PMCA2 (neither PMCA3) protein expression either in control or treated MCF-7 cells using isoform specific antibodies (NR2 and NR3).

3.4. Valerate and PMA induced upregulation of PMCA4b mRNA expression in MCF-7 cells

To support our findings at the protein level we also examined changes in the mRNA expression of PMCA1, 2 and 4 during valerate \pm PMA-induced differentiation of MCF-7 cells (Fig. 3F). The mRNA expression of PMCA1 and PMCA2 was not affected significantly by the treatments, whereas PMCA4 mRNA expression showed marked upregulation (6.7- and 5.4-fold increase in valerate- and PMA-treated cells, respectively, and a large, 34.3-fold increase in valerate plus PMA-treated cells). This correlates well with the enhanced PMCA4b protein expression detected in differentiated MCF-7 cells.

3.5. PKC inhibitor GF 109203X diminished the PMA- but not the valerate-induced upregulation of PMCA4b expression

To gain more insight into the mechanisms of treatments, we supplemented the differentiation-inducing media with the PKC inhibitor GF 109203X hydrochloride to selectively inhibit PKC mediated pathways [54]. Fig. 3G shows that the inhibitor nearly completely abrogated the PMCA4b upregulation induced by PMA, while the PMCA4b expression decreased only slightly in valerate-treated cells. A more pronounced inhibition was observed in cells treated with valerate in combination with PMA, although, no complete inhibition could be detected when valerate was present in the incubation medium. These results suggest that SCFAs and PMA act through different pathways and that PKC is most probably not involved in SCFA-induced PMCA upregulation.

3.6. Subcellular localization of PMCA4b in MCF-7 cells

Previous studies have reported the expression of the PMCA4b isoform in rat mammary gland by RT-PCR [55-57]. Therefore, in most of our studies we used the PMCA4b specific antibody JA3 that recognized specifically the “b” splice variant of PMCA4. To test if the “a” splice variant of PMCA4 was also present in these cells, immunostaining was performed using the PMCA4 antibody JA9 that recognizes both the “a” and “b” variants. Samples overexpressing both splice variants, PMCA4b and PMCA4a, were used as PMCA markers. The Western blots in Fig. 4A clearly demonstrate that the PMCA4b variant is expressed in MCF-7 cells (the upper band in Fig. 4A, lower panel), which is in agreement with previous studies [55-57]. To examine the localization of the upregulated PMCA4b protein, immunocytochemical staining with the isoform and variant specific antibodies (JA9 and JA3, respectively) was performed on valerate ± PMA-treated cells and was analyzed by confocal microscopy (Fig. 4B). PMCA4 expression in the untreated cells was hardly detectable. Under

the same microscope settings, treatment of the cells with valerate or PMA alone increased the PMCA4 signal, and in agreement with the above findings the combined treatment (valerate plus PMA) caused an even higher PMCA4 signal. Moreover, both the PMCA4 (JA9) and PMCA4b (JA3) specific staining showed clear plasma membrane localization so that the newly expressed pump is expected to be functional. The signal intensity of the Na,K ATPase staining did not change significantly upon treatments.

3.7. Effective treatment of cells by SAHA and valproate highlights the importance of histone deacetylase inhibitors in PMCA4b upregulation

Because of the anticancer activity of HDACis, some of them are approved by the Food and Drug Administration (FDA), or they are used in clinical trials either alone or in combination with other drugs [17]. Therefore, we examined whether these inhibitors affected PMCA4b expression in MCF-7 cells. Cells were treated by SAHA and valproate alone or together with PMA, and PMCA expression was followed. Fig. 5 shows that these HDACis, similarly to the SCFAs, remarkably upregulated PMCA4b protein expression (5-10 fold). On the other hand, a slight increase of PMCA1 expression could also be detected. The combined SAHA + PMA or valproate + PMA treatments augmented the PMCA4b upregulation similarly to that seen with valerate. SAHA and valproate further enhanced PMCA4b expression of PMA-treated cells by about two-fold.

3.8. Regulation of Ca²⁺ clearance by PMCA4b in differentiated MCF-7 cells

To study how upregulation of PMCA4b affected Ca²⁺ signaling in breast cancer cells, we established an MCF-7 cell line stably expressing the genetically encoded calcium sensor GCaMP2 (GCaMP2-MCF-7 cells) using the Sleeping Beauty transposon system. A representative image of the GCaMP2-MCF-7 cells is shown in Fig. 6A. The GCaMP2

expressing cells were treated with valerate \pm PMA for 3 days and then fresh medium (without valerate or PMA) was added a day before performing the Ca^{2+} signaling experiments. Fig. 6B indicates that in response to valerate \pm PMA treatments PMCA4b expression was highly elevated (60-600 fold, data not shown) in the GCaMP2-MCF-7 cells similarly to that found in the parental MCF-7 cell line (Fig. 1 and 3). This high level of endogenous PMCA4b expression was comparable with that obtained by transient expression of mCherry-tagged PMCA4b in non-treated GCaMP2-MCF-7 cells.

We performed Ca^{2+} signal measurements by confocal imaging in GCaMP2-MCF-7 cells differentiated with valerate \pm PMA. Before initiating the Ca^{2+} signal the culture medium was replaced with Ca^{2+} free medium, and then intracellular Ca^{2+} pools were discharged by the SERCA-inhibitor thapsigargin (Tg) and the purinergic receptor agonist, ATP. After 5 minutes the external Ca^{2+} was restored to 2 mM and Ca^{2+} influx through store-operated Ca^{2+} channels was followed for an additional 10 minutes. The average relative fluorescence intensities of Ca^{2+} transients in Fig. 6C show that the intracellular Ca^{2+} concentration returned quickly to baseline level in differentiated cells after both ATP-induced stimulus and store operated Ca^{2+} entry (SOCE), while a more sustained Ca^{2+} peak was observed in the untreated control cells. Similarly, when the signal was initiated by the Ca^{2+} ionophore A23187 that evokes Ca^{2+} influx independent of the Ca^{2+} channels, a smaller Ca^{2+} peak was observed in valerate \pm PMA-differentiated cells than in control cells (Fig. 6D). After each experiment cells were fixed and stained with anti-PMCA4 antibody to show that PMCA4b expression was enhanced and the pump was localized correctly after the differentiating treatments. In Fig. 6E representative images of valerate \pm PMA-treated cells are shown after the Ca^{2+} signal measurement. The enhanced Ca^{2+} clearance observed in these experiments is in good agreement with the elevated expression and proper plasma membrane localization of a functional PMCA4b protein in differentiated MCF-7 cells. Based on these results, we can not

rule out the contribution of other Ca^{2+} fluxes, however, the A23187-induced Ca^{2+} signal measurements suggest that changes in the activity of the Ca^{2+} entry channels may not be responsible for the reduced Ca^{2+} signal.

3.9. Regulation of Ca^{2+} clearance in PMCA4b overexpressing MCF-7 cells

To study further the role of PMCA4b in Ca^{2+} signaling we performed Ca^{2+} signal measurements with the GCaMP2-MCF-7 cells transiently transfected with the mCherry-PMCA4x/b construct. Importantly, the level of mCherry-PMCA4x/b overexpression was similar to that of the upregulated endogenous PMCA4b in differentiated cells permitting comparison of the data (Fig. 6B). As demonstrated by the images in Fig. 7A, the mCherry signal helped us identify the PMCA4b overexpressing cells. The diagram in Fig. 7B shows the average relative fluorescence intensities of the Tg- and ATP-induced signals in the absence of extracellular calcium followed by SOCE in mCherry-PMCA4x/b transfected cells. The pattern of the Ca^{2+} signal was very similar to that of the differentiated cells as the intracellular Ca^{2+} concentration returned much faster to the baseline level in PMCA4b overexpressing cells than in the control cells. The half-time from the decay phase of the SOCE transient were determined for each situation (*i.e.* treatments with valerate and PMA and overexpression of the PMCA4b). The bar graph in Fig. 7C shows a significantly shorter half peak decay time of the SOCE transient for cells with an enhanced PMCA4b level than for control cells with much lower PMCA4b expression. Importantly, the half peak decay time of the valerate \pm PMA differentiated cells was comparable to the cells overexpressing mCherry-PMCA4x/b. Also, similarly to the differentiated cells, the A23187-induced Ca^{2+} transient was smaller in the PMCA4b overexpressing cells than in the control cells (Fig. 7D). Thus, overexpression of the PMCA4b protein resulted in similar changes in the Ca^{2+} signaling pattern as the upregulated endogenous pump, suggesting that the PMCA4b protein

endogenously overexpressed during differentiation is critically involved in the Ca^{2+} clearance of differentiated MCF-7 cells and thus contributes to cellular Ca^{2+} homeostasis. However, further studies are needed to assess the impact of each contributor Ca^{2+} channel and pump in the regulation of Ca^{2+} homeostasis of differentiated MCF-7 cells.

3.10. PMCA4 expression in normal breast tissue

PMCA4 expression in normal human breast ductal epithelium was investigated with the JA9 PMCA4-specific monoclonal antibody by immunohistochemistry. As shown in Fig. 8, staining with this antibody led to the labeling of breast ductal epithelial cells. The pattern of PMCA4 staining was compatible with location in the plasma membrane. The detection of PMCA4 in the plasma membrane of normal mammary epithelium indicates that this calcium pump species is involved in calcium homeostasis of normal breast epithelial cells, and that decreased expression in breast carcinoma, as well as induction of expression during cancer cell differentiation are pathophysiologically relevant.

4. Discussion

Remodeling of intracellular Ca^{2+} homeostasis is an important step of tumorigenesis, since intracellular Ca^{2+} signals play role in cell-cycle progression, apoptosis, cell migration and metastasis formation [7, 8]. In breast cancer cells store-operated Ca^{2+} channels are essential for migration and invasion [58], and epithelial-mesenchymal transition can also be regulated through SOCE in MCF-7 cells [59]. Further, SOCE is involved in the apoptosis-inducing effect of butyrate in colon cancer cells [60]. Several lines of evidence suggest that PMCA4s, that are known to reduce intracellular Ca^{2+} concentration after stimuli, are also involved in

the remodeling of Ca²⁺ homeostasis during the differentiation/dedifferentiation process [14, 15, 25, 26].

In this study we investigated the effect of differentiation-inducing agents on the expression and function of PMCAs in MCF-7 cell line. Aberrant HDAC expression initiates tumor progression by causing uncontrolled cell proliferation and blocking the transcription of differentiation and proapoptotic factors [19]. HDACis, which are known differentiating compounds, restore the normal gene expression of cancer cells by altering transcription levels of cell cycle regulatory proteins; they induce the expression of the antiproliferative gene p21, regulate the activity of the tumor suppressor p53, and reduce the expression of positive regulators of proliferation, such as cyclin D1, c-myc and c-Src [17, 18]. The PKC activator PMA directly induces the Raf-MEK-ERK signaling pathway, that further activates the cell-cycle inhibitor p21 and diminishes cell growth [61]. During HDACi- or PMA-induced differentiation we found marked PMCA4b upregulation both at the mRNA and protein levels, while there were no significant changes in the expression of the other PMCA isoforms. PMCA4b expression and differentiation of cells was greatly enhanced when we combined valerate with PMA. Our experiments suggest that these agents act via different mechanisms since PMA-induced PMCA4b upregulation was abrogated by a PKC inhibitor while SCFA-induced upregulation was only slightly modified by PKC inhibition. Similarly to our findings in MCF-7 cells, PMA augmented butyrate-induced differentiation in colon cancer cells but the butyrate-induced differentiation was not inhibited by PKC inhibitors [48]. A more recent study also proves that butyrate-induced cellular processes can be potentiated by PMA. In intestinal epithelial cells SCFAs and PMA activated synergistically the AP-1 transcription factor through the ERK1/2 signaling pathway, which is an important regulator of cell proliferation, differentiation, migration and apoptosis [49]. An interesting finding of this study

was that PMA alone activated the AP-1 through PKC and MEK1/2, while activation by butyrate depended only on MEK1/2.

Correspondingly, expression of SERCA3, a sarco/endoplasmic reticulum-type Ca^{2+} pump is also increased during SCFA-induced differentiation of lung and colon cancer cells [51, 52], indicating that remodeling of Ca^{2+} homeostasis is important in cancer progression and affects more components of the Ca^{2+} handling toolkit. We also found a slight elevation of SERCA3 expression in valerate-treated MCF-7 cells, while PMA induced upregulation of SERCA2.

PMCA2 is a hallmark of the lactating mammary gland but its expression is rapidly downregulated during mammary gland involution, and in non-lactating mammary gland PMCA4b is the major PMCA isoform [55-57]. A recent study showed that elevated PMCA2 expression in mammary epithelial cells inhibited apoptosis and in human breast cancer cases a high PMCA2 mRNA level was associated with poor clinical prognosis [62]. In breast cancer cell lines PMCA1 and PMCA2 was shown to be expressed at an increased level compared to non-tumorigenic cells [11, 12] although, in one study PMCA2 mRNA was not detected by RT-PCR in MCF-7 cells [63]. By real-time quantitative PCR we also observed the expression of all three PMCA isoforms (PMCA1, 2 and 4), however, at the protein level, we found only PMCA1 with some PMCA4 expression in MCF-7 cells. By using an isoform specific antibody which clearly recognized overexpressed PMCA2b in COS-7 cells, we could not detect any PMCA2 protein expression in MCF-7 cells.

PMCA2s are needed to restore the low level of intracellular Ca^{2+} concentration after stimulus and thus, changes in their expression could substantially alter the amplitude and duration of the Ca^{2+} signal. Our studies show a remarkable enhancement of PMCA4b expression during the differentiation of MCF-7 cells induced by a combined treatment with valerate and PMA; the PMCA4b mRNA level showed more than 30-fold elevation while the

protein expression increased over 500-fold. Moreover, the overall PMCA content (PMCA1 and 4) of cells was increased more than 10-fold.

SAHA and valproate, which are FDA-approved epigenetic drugs, also induced PMCA4b upregulation in our experiments. SAHA (Vorinostat) is a currently approved agent against cutaneous T-cell lymphoma, and clinical trials are ongoing against breast cancer and other solid tumors or hematological malignancies [17, 64]. Valproate was used primarily as an anticonvulsant and mood-stabilizing drug, but now, mostly in combination with other therapeutic agents, it is being tested in clinical studies for cancer treatment [17, 65]. Modulation of PMCA expression during HDACi-treatments may be an important step in the mode of action of these anticancer agents.

Further confocal imaging studies showed that the newly synthesized pump is located mainly in the plasma membrane and therefore is expected to be functional. In good correlation with the increased plasma membrane expression of the pump we detected enhanced Ca^{2+} clearance from stimulated MCF-7 cells. Similarly, when PMCA4b was overexpressed in non-treated MCF-7 cells, the Ca^{2+} signal returned more quickly to the baseline level than in the control cells, underlining the importance of PMCA4b in Ca^{2+} clearance from the differentiated cells.

The role of PMCA4 in Ca^{2+} signaling has been studied in several other cancer cell lines using an siRNA silencing approach. Knocking down PMCA4 intensified the agonist-induced Ca^{2+} signal in HT-29 colon cancer cells [14]. However, when individual PMCA isoforms were knocked down in MDA-MB-231 breast cancer cells, silencing of PMCA4 did not change the Ca^{2+} signals evoked by different agents. In these cells PMCA1 silencing, on the other hand, markedly altered Ca^{2+} signaling indicating that PMCA1 was the main regulator of global Ca^{2+} signals [66] in undifferentiated cells.

PMCA4b is also known to interact with several signal and scaffold proteins which may connect this PMCA variant to specific signalling pathways [2]. As an example, the second intracellular loop of PMCA4b was shown to interact with the proapoptotic tumor suppressor RASSF1 that may negatively regulate the EGF-induced ERK activation [67]. Calcineurin, a regulator of NFAT signaling, was also found to bind to PMCA4b that resulted in suppressed NFAT transcription in HEK293 cells [68]. On the other hand, PMCA4b binding to the α -1 syntrophin and nitric oxide synthase I can form a ternary complex, that modulates NO production and signaling in mouse heart tissue [68], in cerebellar granule cells [69, 70] and in osteoclast differentiation [71]. Through the C-terminal tail, PMCA4b can bind to several PDZ proteins, such as SAP90/PSD95, SAP97, SAP102 [72], the Ania-3/Homer scaffold protein [73], that may arrange PMCA into specific membrane domains to regulate local Ca^{2+} signaling. More recently, PMCA4 was shown to interact with STIM1 that influenced T-cell activation through the activation of NFAT [74].

Importantly, PMCA4 expression could be detected in normal, fully differentiated breast epithelial tissue indicating that PMCA4b is an essential element of the Ca^{2+} homeostasis and probably other signalling pathways of the fully differentiated breast epithelium. These data together with the selective upregulation of PMCA4b expression during the differentiation of MCF-7 cells suggest that PMCA4b is connected to the differentiation program; and consequently, insufficient PMCA4b expression may contribute to the development and/or further progression of breast tumors. Remodeling of Ca^{2+} homeostasis in cancer cells is a hallmark of tumor progression and our findings support the idea that PMCA4b is essentially involved in that process.

Acknowledgements

We are grateful to Krisztina Lór for the excellent technical assistance. We thank Tamás Orbán and Anita Schamberger for their help in the real-time PCR analysis. We are much obliged to Tamás Orbán (Institute of Molecular Pharmacology, Research Centre for Natural Sciences, Hungarian Academy of Sciences) for providing the SB-CAG-GCaMP2-CAG-Puro and the SB100× transposase constructs. This work was supported by grants from the Hungarian Scientific Research Fund (OTKA CK 80283, K 101064 to A.E.); the Hungarian Ministry of National Development (“TransRat” KMR_12-1-2012-0112 and KTIA_AIK_12-1-2012-0025); and by the Association pour la Recherche sur le Cancer, France and Inserm (to B.P.).

References

- [1] M. Brini, E. Carafoli, Calcium pumps in health and disease, *Physiol. Rev.*, 89 (2009) 1341-1378.
- [2] E.E. Strehler, A.J. Caride, A.G. Filoteo, Y. Xiong, J.T. Penniston, A. Enyedi, Plasma membrane Ca^{2+} ATPases as dynamic regulators of cellular calcium handling, *Ann. N. Y. Acad. Sci.*, 1099 (2007) 226-236.
- [3] E. Strehler, D. Zacharias, Role of alternative splicing in generating isoform diversity among plasma membrane calcium pumps, *Physiol. Rev.*, 81 (2001) 21-50.
- [4] F. Di Leva, T. Domi, L. Fedrizzi, D. Lim, E. Carafoli, The plasma membrane Ca^{2+} ATPase of animal cells: structure, function and regulation, *Arch. Biochem. Biophys.*, 476 (2008) 65-74.
- [5] H. Roderick, S. Cook, Ca^{2+} signalling checkpoints in cancer: remodelling Ca^{2+} for cancer cell proliferation and survival, *Nat. Rev. Cancer*, 8 (2008) 361-375.
- [6] J. Parkash, K. Asotra, Calcium wave signaling in cancer cells, *Life Sci.*, 87 (2010) 587-595.
- [7] N. Prevarskaya, R. Skryma, Y. Shuba, Ion channels and the hallmarks of cancer, *Trends Mol. Med.*, 16 (2010) 107-121.
- [8] G. Monteith, F. Davis, S. Roberts-Thomson, Calcium channels and pumps in cancer: changes and consequences, *J. Biol. Chem.*, 287 (2012) 31666-31673.
- [9] S. Roberts-Thomson, M. Curry, G. Monteith, Plasma membrane calcium pumps and their emerging roles in cancer, *World. J. Biol. Chem.*, 1 (2010) 248-253.
- [10] P. Reisner, P. Brandt, T. Vanaman, Analysis of plasma membrane Ca^{2+} -ATPase expression in control and SV40-transformed human fibroblasts, *Cell Calcium*, 21 (1997) 53-62.

- [11] W. Lee, S. Roberts-Thomson, N. Holman, F. May, G. Lehrbach, G. Monteith, Expression of plasma membrane calcium pump isoform mRNAs in breast cancer cell lines, *Cell. Signal.*, 14 (2002) 1015-1022.
- [12] W. Lee, S. Roberts-Thomson, G. Monteith, Plasma membrane calcium-ATPase 2 and 4 in human breast cancer cell lines, *Biochem. Biophys. Res. Commun.*, 337 (2005) 779-783.
- [13] K. Saito, K. Uzawa, Y. Endo, Y. Kato, D. Nakashima, K. Ogawara, M. Shiba, H. Bukawa, H. Yokoe, H. Tanzawa, Plasma membrane Ca^{2+} ATPase isoform 1 down-regulated in human oral cancer, *Oncol. Rep.*, 15 (2006) 49-55.
- [14] C. Aung, W. Ye, G. Plowman, A. Peters, G. Monteith, S. Roberts-Thomson, Plasma membrane calcium ATPase 4 and the remodeling of calcium homeostasis in human colon cancer cells, *Carcinogenesis*, 30 (2009) 1962-1969.
- [15] J. Rüschoff, T. Brandenburger, E. Strehler, A. Filoteo, E. Heinmöller, G. Aumüller, B. Wilhelm, Plasma membrane calcium ATPase expression in human colon multistep carcinogenesis, *Cancer Invest.*, 30 (2012) 251-257.
- [16] Y.M. Usachev, L.T. Sonja, M.G. Geoffrey, E.S. Emanuel, A.T. Stanley, Differentiation induces up-regulation of plasma membrane Ca^{2+} -ATPase and concomitant increase in Ca^{2+} efflux in human neuroblastoma cell line IMR-32, *J. Neurochem.*, 76 (2001).
- [17] C. Dell'Aversana, I. Lepore, L. Altucci, HDAC modulation and cell death in the clinic, *Exp. Cell Res.*, 318 (2012) 1229-1244.
- [18] M. Dickinson, R. Johnstone, H. Prince, Histone deacetylase inhibitors: potential targets responsible for their anti-cancer effect, *Invest. New Drugs*, 28 Suppl 1 (2010) 20.
- [19] M. Glozak, E. Seto, Histone deacetylases and cancer, *Oncogene*, 26 (2007) 5420-5432.
- [20] Y. Drabsch, R. Robert, T. Gonda, MYB suppresses differentiation and apoptosis of human breast cancer cells, *Breast Cancer Res.*, 12 (2010).

- [21] N. Guilbaud, N. Gas, M. Dupont, A. Valette, Effects of differentiation-inducing agents on maturation of human MCF-7 breast cancer cells, *J. Cell. Physiol.*, 145 (1990) 162-172.
- [22] O. Nayler, A. Hartmann, S. Stamm, The ER repeat protein YT521-B localizes to a novel subnuclear compartment, *J. Cell Biol.*, 150 (2000) 949-962.
- [23] S. Siavoshian, H. Blottière, E. Le Foll, B. Kaeffer, C. Cherbut, J. Galmiche, Comparison of the effect of different short chain fatty acids on the growth and differentiation of human colonic carcinoma cell lines in vitro, *Cell Biol. Int.*, 21 (1997) 281-287.
- [24] B.F. Hinnebusch, S. Meng, J.T. Wu, S.Y. Archer, R.A. Hodin, The effects of short-chain fatty acids on human colon cancer cell phenotype are associated with histone hyperacetylation, *J. Nutr.*, 132 (2002) 1012-1017.
- [25] P. Ribiczey, A. Tordai, H. Andrikovics, A. Filoteo, J. Penniston, J. Enouf, A. Enyedi, B. Papp, T. Kovács, Isoform-specific up-regulation of plasma membrane Ca^{2+} ATPase expression during colon and gastric cancer cell differentiation, *Cell Calcium*, 42 (2007) 590-605.
- [26] C. Aung, W. Kruger, P. Poronnik, S. Roberts-Thomson, G. Monteith, Plasma membrane Ca^{2+} -ATPase expression during colon cancer cell line differentiation, *Biochem. Biophys. Res. Commun.*, 355 (2007) 932-936.
- [27] T. Kuo, K. Wang, L. Carlock, C. Diglio, W. Tsang, Phorbol ester induces both gene expression and phosphorylation of the plasma membrane Ca^{2+} pump, *J. Biol. Chem.*, 266 (1991) 2520-2525.
- [28] G. Antalffy, K. Paszty, K. Varga, L. Hegedus, A. Enyedi, R. Padanyi, A C-terminal dileucine motif controls plasma membrane expression of PMCA4b, *Biochim. Biophys. Acta*, 1833 (2013) 2561-2572.
- [29] Z. Ivics, P. Hackett, R. Plasterk, Z. Izsvák, Molecular reconstruction of Sleeping Beauty, a Tc1-like transposon from fish, and its transposition in human cells, *Cell*, 91 (1997) 501-510.

- [30] Z. Izsvák, M. Chuah, T. Vandendriessche, Z. Ivics, Efficient stable gene transfer into human cells by the Sleeping Beauty transposon vectors, *Methods*, 49 (2009) 287-297.
- [31] A. Apáti, K. Pászty, L. Hegedűs, O. Kolacsek, T. Orbán, Z. Erdei, K. Szebényi, A. Péntek, A. Enyedi, B. Sarkadi, Characterization of calcium signals in human embryonic stem cells and in their differentiated offspring by a stably integrated calcium indicator protein, *Cell. Signal.*, 25 (2013) 752-759.
- [32] R. Padányi, K. Pászty, E. Strehler, A. Enyedi, PSD-95 mediates membrane clustering of the human plasma membrane Ca^{2+} pump isoform 4b, *Biochim. Biophys. Acta*, 1793 (2009) 1023-1032.
- [33] A. Caride, A. Filoteo, A. Enyedi, A. Verma, J. Penniston, Detection of isoform 4 of the plasma membrane calcium pump in human tissues by using isoform-specific monoclonal antibodies, *Biochem. J.*, 316 (Pt 1) (1996) 353-359.
- [34] A. Filoteo, N. Elwess, A. Enyedi, A. Caride, H. Aung, J. Penniston, Plasma membrane Ca^{2+} pump in rat brain. Patterns of alternative splices seen by isoform-specific antibodies, *J. Biol. Chem.*, 272 (1997) 23741-23747.
- [35] H.D. Soule, J. Vazquez, A. Long, S. Albert, M. Brennan, A human cell line from a pleural effusion derived from a breast carcinoma, *J. Natl. Cancer Inst.*, 51 (1973) 1409-1416.
- [36] J. Chen, F. Ghazawi, W. Bakkar, Q. Li, Valproic acid and butyrate induce apoptosis in human cancer cells through inhibition of gene expression of Akt/protein kinase B, *Mol. Cancer*, 5 (2006) 71.
- [37] B. Heerdt, M. Houston, G. Anthony, L. Augenlicht, Initiation of growth arrest and apoptosis of MCF-7 mammary carcinoma cells by tributyrin, a triglyceride analogue of the short-chain fatty acid butyrate, is associated with mitochondrial activity, *Cancer Res.*, 59 (1999) 1584-1591.

- [38] M. Mandal, R. Kumar, Bcl-2 expression regulates sodium butyrate-induced apoptosis in human MCF-7 breast cancer cells, *Cell Growth Differ.*, 7 (1996) 311-318.
- [39] G.M. Matthews, G.S. Howarth, R.N. Butler, Short-chain fatty acid modulation of apoptosis in the Kato III human gastric carcinoma cell line, *Cancer Biol. Ther.*, 6 (2007) 1051-1057.
- [40] F. Natoni, L. Diolordi, C. Santoni, M. Gilardini Montani, Sodium butyrate sensitises human pancreatic cancer cells to both the intrinsic and the extrinsic apoptotic pathways, *Biochim. Biophys. Acta*, 1745 (2005) 318-329.
- [41] J.-C. Lee, M.-C. Maa, H.-S. Yu, J.-H. Wang, C.-K. Yen, S.-T. Wang, Y.-J. Chen, Y. Liu, Y.-T. Jin, T.-H. Leu, Butyrate regulates the expression of c-Src and focal adhesion kinase and inhibits cell invasion of human colon cancer cells, *Mol. Carcinog.*, 43 (2005) 207-214.
- [42] J. de Vente, C. Kukoly, W. Bryant, K. Posekany, J. Chen, D. Fletcher, P. Parker, G. Pettit, G. Lozano, P. Cook, Phorbol esters induce death in MCF-7 breast cancer cells with altered expression of protein kinase C isoforms. Role for p53-independent induction of gadd-45 in initiating death, *J. Clin. Invest.*, 96 (1995) 1874-1886.
- [43] M. Shanmugam, N. Krett, E. Maizels, F. Murad, S. Rosen, M. Hunzicker-Dunn, A role for protein kinase C delta in the differential sensitivity of MCF-7 and MDA-MB 231 human breast cancer cells to phorbol ester-induced growth arrest and p21(WAF1/CIP1) induction, *Cancer Lett.*, 172 (2001) 43-53.
- [44] V. Fortino, C. Torricelli, E. Capurro, G. Sacchi, G. Valacchi, E. Maioli, Antiproliferative and survival properties of PMA in MCF-7 breast cancer cell, *Cancer Invest.*, 26 (2008) 13-21.
- [45] C. Nunes-Xavier, C. Tárrega, R. Cejudo-Marín, J. Frijhoff, A. Sandin, A. Ostman, R. Pulido, Differential up-regulation of MAP kinase phosphatases MKP3/DUSP6 and DUSP5 by Ets2 and c-Jun converge in the control of the growth arrest versus proliferation response of MCF-7 breast cancer cells to phorbol ester, *J. Biol. Chem.*, 285 (2010) 26417-26430.

- [46] A. Urtreger, M. Kazanietz, E. Bal de Kier Joffé, Contribution of individual PKC isoforms to breast cancer progression, *IUBMB Life*, 64 (2012) 18-26.
- [47] H. You, W. Yu, B. Sanders, K. Kline, RRR-alpha-tocopheryl succinate induces MDA-MB-435 and MCF-7 human breast cancer cells to undergo differentiation, *Cell Growth Differ.*, 12 (2001) 471-480.
- [48] K. Rickard, P. Gibson, G. Young, W. Phillips, Activation of protein kinase C augments butyrate-induced differentiation and turnover in human colonic epithelial cells in vitro, *Carcinogenesis*, 20 (1999) 977-984.
- [49] M. Nepelska, A. Cultrone, F. Béguet-Crespel, K. Le Roux, J. Doré, V. Arulampalam, H. Blottière, Butyrate produced by commensal bacteria potentiates phorbol esters induced AP-1 response in human intestinal epithelial cells, *PloS One*, 7 (2012) e52869.
- [50] B. Papp, J.-P. Brouland, Altered Endoplasmic Reticulum Calcium Pump Expression during Breast Tumorigenesis, *Breast Cancer (Auckl.)*, 5 (2011) 163-174.
- [51] P. Gélébart, T. Kovács, J.-P. Brouland, R. van Gorp, J. Grossmann, N. Rivard, Y. Panis, V. Martin, R. Bredoux, J. Enouf, B. Papp, Expression of endomembrane calcium pumps in colon and gastric cancer cells. Induction of SERCA3 expression during differentiation, *J. Biol. Chem.*, 277 (2002) 26310-26320.
- [52] A. Arbabian, J.P. Brouland, A. Apati, K. Paszty, L. Hegedus, A. Enyedi, C. Chomienne, B. Papp, Modulation of endoplasmic reticulum calcium pump expression during lung cancer cell differentiation, *FEBS J.*, 280 (2013) 5408-5418.
- [53] W. Lee, J. Robinson, N. Holman, M. McCall, S. Roberts-Thomson, G. Monteith, Antisense-mediated Inhibition of the plasma membrane calcium-ATPase suppresses proliferation of MCF-7 cells, *J. Biol. Chem.*, 280 (2005) 27076-27084.

- [54] D. Toullec, P. Pianetti, H. Coste, P. Bellevergue, T. Grand-Perret, M. Ajakane, V. Baudet, P. Boissin, E. Boursier, F. Loriolle, The bisindolylmaleimide GF 109203X is a potent and selective inhibitor of protein kinase C, *J. Biol. Chem.*, 266 (1991) 15771-15781.
- [55] T. Reinhardt, J. Lippolis, Mammary gland involution is associated with rapid down regulation of major mammary Ca^{2+} -ATPases, *Biochem. Biophys. Res. Commun.*, 378 (2009) 99-102.
- [56] T.A. Reinhardt, A.G. Filoteo, J.T. Penniston, R.L. Horst, Ca^{2+} -ATPase protein expression in mammary tissue, *Am. J. Physiol.-Cell Ph.*, 279 (2000) C1595-1602.
- [57] T.A. Reinhardt, R.L. Horst, Ca^{2+} -ATPases and their expression in the mammary gland of pregnant and lactating rats, *The American journal of physiology*, 276 (1999) C796-802.
- [58] S. Yang, J. Zhang, X.-Y. Huang, Orai1 and STIM1 are critical for breast tumor cell migration and metastasis, *Cancer cell*, 15 (2009) 124-134.
- [59] J. Hu, K. Qin, Y. Zhang, J. Gong, N. Li, D. Lv, R. Xiang, X. Tan, Downregulation of transcription factor Oct4 induces an epithelial-to-mesenchymal transition via enhancement of Ca^{2+} influx in breast cancer cells, *Biochem. Biophys. Res. Commun.*, 411 (2011) 786-791.
- [60] S. Sun, W. Li, H. Zhang, L. Zha, Y. Xue, X. Wu, F. Zou, Requirement for store-operated calcium entry in sodium butyrate-induced apoptosis in human colon cancer cells, *Biosci. Rep.*, 32 (2012) 83-90.
- [61] K. Moelling, K. Schad, M. Bosse, S. Zimmermann, M. Schweneker, Regulation of Raf-Akt Cross-talk, *J. Biol. Chem.*, 277 (2002) 31099-31106.
- [62] J. VanHouten, C. Sullivan, C. Bazinet, T. Ryoo, R. Camp, D. Rimm, G. Chung, J. Wysolmerski, PMCA2 regulates apoptosis during mammary gland involution and predicts outcome in breast cancer, *Proc. Natl. Acad. Sci. U. S. A.*, 107 (2010) 11405-11410.
- [63] U. Anantamongkol, H. Takemura, T. Suthiphongchai, N. Krishnamra, Y. Horio, Regulation of Ca^{2+} mobilization by prolactin in mammary gland cells: possible role of

secretory pathway Ca^{2+} -ATPase type 2, *Biochem. Biophys. Res. Commun.*, 352 (2007) 537-542.

[64] P.N. Munster, K.T. Thurn, S. Thomas, P. Raha, M. Lacevic, A. Miller, M. Melisko, R. Ismail-Khan, H. Rugo, M. Moasser, S.E. Minton, A phase II study of the histone deacetylase inhibitor vorinostat combined with tamoxifen for the treatment of patients with hormone therapy-resistant breast cancer, *Br. J. Cancer*, 104 (2011) 1828-1835.

[65] A. Duenas-Gonzalez, M. Candelaria, C. Perez-Plascencia, E. Perez-Cardenas, E. de la Cruz-Hernandez, L. Herrera, Valproic acid as epigenetic cancer drug: preclinical, clinical and transcriptional effects on solid tumors, *Cancer Treat. Rev.*, 34 (2008) 206-222.

[66] M. Curry, N. Luk, P. Kenny, S. Roberts-Thomson, G. Monteith, Distinct regulation of cytoplasmic calcium signals and cell death pathways by different plasma membrane calcium ATPase isoforms in MDA-MB-231 breast cancer cells, *J. Biol. Chem.*, 287 (2012) 28598-28608.

[67] A. Armesilla, J. Williams, M. Buch, A. Pickard, M. Emerson, E. Cartwright, D. Oceandy, M. Vos, S. Gillies, G. Clark, L. Neyses, Novel functional interaction between the plasma membrane Ca^{2+} pump 4b and the proapoptotic tumor suppressor Ras-associated factor 1 (RASSF1), *J. Biol. Chem.*, 279 (2004) 31318-31328.

[68] M. Buch, A. Pickard, A. Rodriguez, S. Gillies, A. Maass, M. Emerson, E. Cartwright, J. Williams, D. Oceandy, J. Redondo, L. Neyses, A. Armesilla, The sarcolemmal calcium pump inhibits the calcineurin/nuclear factor of activated T-cell pathway via interaction with the calcineurin A catalytic subunit, *J. Biol. Chem.*, 280 (2005) 29479-29487.

[69] J.C. Williams, A.L. Armesilla, T.M. Mohamed, C.L. Hagarty, F.H. McIntyre, S. Schomburg, A.O. Zaki, D. Oceandy, E.J. Cartwright, M.H. Buch, M. Emerson, L. Neyses, The sarcolemmal calcium pump, alpha-1 syntrophin, and neuronal nitric-oxide synthase are parts of a macromolecular protein complex, *J. Biol. Chem.*, 281 (2006) 23341-23348.

- [70] W. Duan, J. Zhou, W. Li, T. Zhou, Q. Chen, F. Yang, T. Wei, Plasma membrane calcium ATPase 4b inhibits nitric oxide generation through calcium-induced dynamic interaction with neuronal nitric oxide synthase, *Protein & cell*, 4 (2013) 286-298.
- [71] H. Kim, V. Prasad, S.-W. Hyung, Z. Lee, S.-W. Lee, A. Bhargava, D. Pearce, Y. Lee, H.-H. Kim, Plasma membrane calcium ATPase regulates bone mass by fine-tuning osteoclast differentiation and survival, *J. Cell Biol.*, 199 (2012) 1145-1158.
- [72] S. DeMarco, E. Strehler, Plasma membrane Ca^{2+} -atpase isoforms 2b and 4b interact promiscuously and selectively with members of the membrane-associated guanylate kinase family of PDZ (PSD95/Dlg/ZO-1) domain-containing proteins, *J. Biol. Chem.*, 276 (2001) 21594-21600.
- [73] V. Sgambato-Faure, Y. Xiong, J.D. Berke, S.E. Hyman, E.E. Strehler, The Homer-1 protein Ania-3 interacts with the plasma membrane calcium pump, *Biochem. Biophys. Res. Commun.*, 343 (2006) 630-637.
- [74] M. Ritchie, E. Samakai, J. Soboloff, STIM1 is required for attenuation of PMCA-mediated Ca^{2+} clearance during T-cell activation, *The EMBO journal*, 31 (2012) 1123-1133.

Figure legends

Fig. 1. SCFAs and PMA induce upregulation of PMCA4b protein expression in MCF-7 cells. (A-D) Concentration dependent effects of treatments. MCF-7 cells were treated with the indicated amounts of butyrate (A), phenylbutyrate (B), valerate (C) or PMA (D) for 5 days, and PMCA protein expression from total cell lysates (20 μ g protein per sample) was analyzed by Western blotting with anti-*pan* PMCA (5F10), anti-PMCA1 (PA1-914) and anti-PMCA4b (JA3) antibodies. Na,K-ATPase served as a loading control. A mixed sample was loaded onto the gels as a positive control. This consisted of microsomal membrane protein obtained from COS-7 cells (1 μ g; this marked the position of PMCA1) mixed with microsomal membrane protein from COS-7 cells transfected with the PMCA4b constructs (0.05 μ g; this marked PMCA4b). (E) Time course of PMCA4b expression during different treatments (5 mM butyrate, phenylbutyrate (PB) or valerate, or 10 nM PMA as indicated) for up to 5 days. (F-G) Densitometric analysis of PMCA4b (F) and total PMCA (G) expression after a 5 day treatment. Data were normalized to the expression levels of Na,K-ATPase and expressed as fold increase over the untreated controls. Bars represent means \pm SD from three to five independent experiments.

Fig. 2. SCFA and PMA treatments inhibit cell proliferation, and induce differentiation of MCF-7 cells. (A-B) Effects of treatments on proliferation. (A) Equal numbers of MCF-7 cells were treated with the indicated amounts of compounds, and numbers of viable cells were counted after 4 days of treatments. Values are means \pm SD from two independent experiments, each having three replicates. (B) Time course of proliferation after 2 mM valerate \pm 10 nM PMA treatments. (C-E) Effects of treatments on differentiation. (C) Cells were treated with the indicated differentiating agents for 4 days and lipid droplets were

stained with Oil Red O. Oil Red O fluorescence was analyzed by using the ImageJ software. Total areas of lipid droplets per total cell numbers were calculated. Bars represent means \pm SD of eight representative pictures per treatment from two independent experiments. Significance is denoted by *** ($P < 0.001$); two-tailed unpaired t-test. (D) Time course of differentiation after 2 mM valerate \pm 10 nM PMA treatments. (E) Representative phase contrast and fluorescent images of 2 mM valerate \pm 10 nM PMA-treated cells.

Fig 3. Treatment with valerate in combination with PMA further increases the expression of PMCA4b. (A) Immunoblots of valerate \pm PMA-treated cells. MCF-7 cells were treated with 2 mM valerate or 10 nM PMA alone, or with 2 mM valerate in combination with 10 nM PMA up to 3 days. Equal amounts of cell lysates (15 μ g of protein) were analyzed by Western blot. PMCA and SERCA expressions were determined using anti-pan PMCA (5F10), anti-PMCA4b (JA3), anti-SERCA2 (IID8) or anti-SERCA3 (PL/IM430) antibodies. Na,K-ATPase served as a loading control. (B-C) Densitometric analysis of PMCA4b (B) and total PMCA (C) expression after 3 days of treatment. Data were normalized to the expression levels of Na,K-ATPase and expressed as fold increase over the untreated controls. Bars represent means \pm SD from five independent experiments. (D) Time course of PMCA4b expression. Values represent means \pm SD from two independent experiments. (E) Detection of different PMCA isoforms by immunoprecipitation. Cells were treated with 2 mM valerate \pm 10 nM PMA for 4 days, then lysed and proteins were immunoprecipitated with an anti-pan PMCA antibody (5F10). PMCA isoform expression was further analyzed by Western blot with isoform-specific antibodies. Equal volumes of input (7.5 μ l) and immunoprecipitated samples (15 μ l) were loaded onto the gel and proteins were detected with specific antibodies for all PMCA isoforms (NR1, NR2, NR3 and JA3 for PMCA1, 2, 3 and 4, respectively). Microsomal membrane preparations isolated from COS-7 cells were used as isoform-specific

positive controls. For PMCA1 the endogenous protein expression was detected (1 μg of microsomal membrane protein) while in the case of the other PMCA isoforms COS-7 cells were transiently transfected with the PMCA2, PMCA3 or PMCA4b constructs and 0.5 μg (for PMCA2 and 3) or 0.05 μg (for PMCA4b) of microsomal membrane protein were loaded onto the gel. (F) Relative mRNA expression of PMCA isoforms in 2 mM valerate \pm 10 nM PMA-treated cells. All data are expressed as fold change in mRNA levels relative to the untreated controls after normalization to RPLP0 and POLR2A endogenous reference genes. Bars represent means \pm SD from three independent experiments, each having three technical replicates. Significances between untreated control cells and treated cells are denoted by ** ($P < 0.01$), * ($P < 0.05$) or n.s. (not significant); two-tailed paired t-test. (G) Effects of PKC inhibitor treatment on PMCA4b upregulation in valerate \pm PMA-treated cells. Cells were pretreated with 1 μM GF 109203X 1 hour before the addition of valerate and/or PMA, and after 4 days of treatment PMCA4b expression from total cell lysates (10 μg protein per sample) was analyzed by Western blotting with antibody JA3. In order to make the inhibition visible in each case, control samples (expressing much lower amounts of PMCA4b) were developed with a longer exposure time while valerate + PMA-treated samples were developed with a shorter exposure time than valerate- or PMA-treated samples. Inhibition is expressed as percent of original. Data are mean \pm SD of densitometrically analyzed Western blots from two independent experiments.

Fig. 4. (A) Upregulation of PMCA4 is specific for the PMCA4b isoform. Total cell lysates (10 μg protein per sample) from valerate \pm PMA-treated cells were analyzed by Western blotting with anti-PMCA4b (JA3) and anti-PMCA4 (JA9) antibodies. A mixed sample of microsomal membrane protein obtained from COS-7 cells transfected with the PMCA4a construct (0.25 μg) and with the PMCA4b construct (0.05 μg) was loaded onto the gels as a

positive control. (B) PMCA4b shows clear plasma membrane localization. Cells were treated with 2 mM valerate \pm 10 nM PMA for 4 days, then cells were immunostained with either anti-PMCA4b (JA3) or anti-PMCA4 (JA9) and anti-Na,K-ATPase antibodies, and images were taken by confocal microscopy. Scale bar, 50 μ m.

Fig. 5. SAHA and valproate (VPA) induce upregulation of PMCA4b protein expression in MCF-7 cells. (A and C) Concentration-dependent effects of treatments. Cells were treated with the indicated amounts of SAHA (A) or VPA (C) alone, or in combination with 10 nM PMA for 4 days, and protein expression from total cell lysates (10 μ g protein per sample) was analyzed by Western blotting with anti-PMCA4b (JA3) and anti-PMCA1 (PA1-914) antibodies. Na,K-ATPase served as a loading control, as above. (B and D) Densitometric analysis for PMCA4b expression after SAHA (B) or VPA (D) treatments. Data were normalized to the expression levels of Na,K-ATPase and expressed as fold increase over the untreated controls. Bars represent means \pm SD from three independent experiments.

Fig. 6. Enhanced PMCA4b expression diminishes intracellular Ca^{2+} signaling in differentiated GCaMP2-MCF-7 cells. (A) MCF-7 cells were stably transfected with the GCaMP2 Ca^{2+} sensor (GCaMP2-MCF-7 cells) and Ca^{2+} signals were detected by confocal microscopy. (B) Western blot analysis of PMCA4b expression from whole cell lysates of GCaMP2-MCF-7 cells. Cells were either differentiated with the indicated amounts of compounds or transiently transfected with the mCherry-PMCA4x/b construct, and equal amounts of cell lysates (5 μ g of protein) were loaded onto the gel. Expression of PMCA4b was analyzed with an anti-PMCA4b antibody (JA3). Na,K-ATPase served as a loading control. (C) Ca^{2+} signal measurements in differentiated GCaMP2-MCF-7 cells. Cells were treated with 2 mM valerate alone or in combination with 10 nM PMA for 3 days, then the medium was replaced by fresh

DMEM and cells were incubated in the absence of differentiating compounds for an additional 24 hours. To test Ca^{2+} signaling using internal sources of Ca^{2+} the culture medium was replaced by Ca^{2+} free HBSS and intracellular stores were challenged by the addition of 2 μM thapsigargin (Tg) and 100 μM ATP, as indicated. After 5 minutes the external Ca^{2+} was restored to 2mM and Ca^{2+} influx through store-operated Ca^{2+} channels was followed for another 10 minutes by confocal imaging. Data represent means of normalized values (F/F_0) \pm 95% CI of about 50 to 70 cells collected from three independent experiments. (D) Intracellular Ca^{2+} signals evoked by the Ca^{2+} ionophore A23187 in valerate \pm PMA treated GCaMP2-MCF-7 cells. Before initiating the Ca^{2+} signal, culture medium was replaced by HBSS supplemented with 2 mM Ca^{2+} and Ca^{2+} influx was triggered by A23187, as indicated. Data represent means of normalized values (F/F_0) \pm 95% CI of about 15 to 25 cells. (E) Representative confocal images of PMCA4 expression in GCaMP2-MCF-7 cells after the Ca^{2+} signal measurement. Cells were fixed and immunostained with anti-PMCA4 antibody (JA9). Scale bar, 50 μm .

Fig. 7. Overexpression of mCherry-PMCA4x/b leads to increased Ca^{2+} clearance after stimulation in GCaMP2-MCF-7 cells. (A) Representative confocal images of mCherry-PMCA4x/b expression in transiently transfected GCaMP2-MCF-7 cells. Scale bar, 20 μm . (B) Ca^{2+} signaling in GCaMP2-MCF-7 cells transiently expressing the mCherry-PMCA4x/b construct. Before initiating the Ca^{2+} signal, culture medium was replaced by Ca^{2+} free HBSS, and then 2 μM thapsigargin (Tg) and 100 μM ATP were added. After 5 minutes of incubation, when the internal Ca^{2+} stores were depleted, external Ca^{2+} was restored to 2mM, and Ca^{2+} influx was followed for another 10 minutes. Data represent means of normalized values (F/F_0) \pm 95% CI of about 25 to 40 cells from four independent experiments. (C) Half peak decay time of the second phase of the transients (SOCE) in differentiated and mCherry-PMCA4x/b

overexpressing cells. Bar graphs are means \pm SD from three or four independent experiments. Significances between control and PMCA4b expressing cells are denoted by * ($P < 0.05$); two-tailed unpaired t-test. (D) Intracellular Ca^{2+} signals evoked by the Ca^{2+} ionophore A23187 in mCherry-PMCA4x/b transfected GCaMP2-MCF-7 cells. Before initiating the Ca^{2+} signal, culture medium was replaced by HBSS supplemented with 2 mM Ca^{2+} and Ca^{2+} influx was triggered by A23187, as indicated. Data represent means of normalized values (F/F_0) \pm 95% CI of about 10 cells.

Fig. 8. Immunohistochemical detection of PMCA4 in normal breast tissue. Tissue sections from archival normal human mammary gland specimens were stained with the anti-PMCA4 antibody (JA9), and signal was visualized using an indirect avidin-biotin-peroxydase detection system with 3,3'-diaminobenzidine as chromogen. Slides were counterstained with hematoxylin. Brown staining in mammary ductal epithelium indicates PMCA4 expression in a plasma membrane location. A representative image of four different samples is shown. Staining with isotype-matched negative control antibody was negative.

FIGURE 1

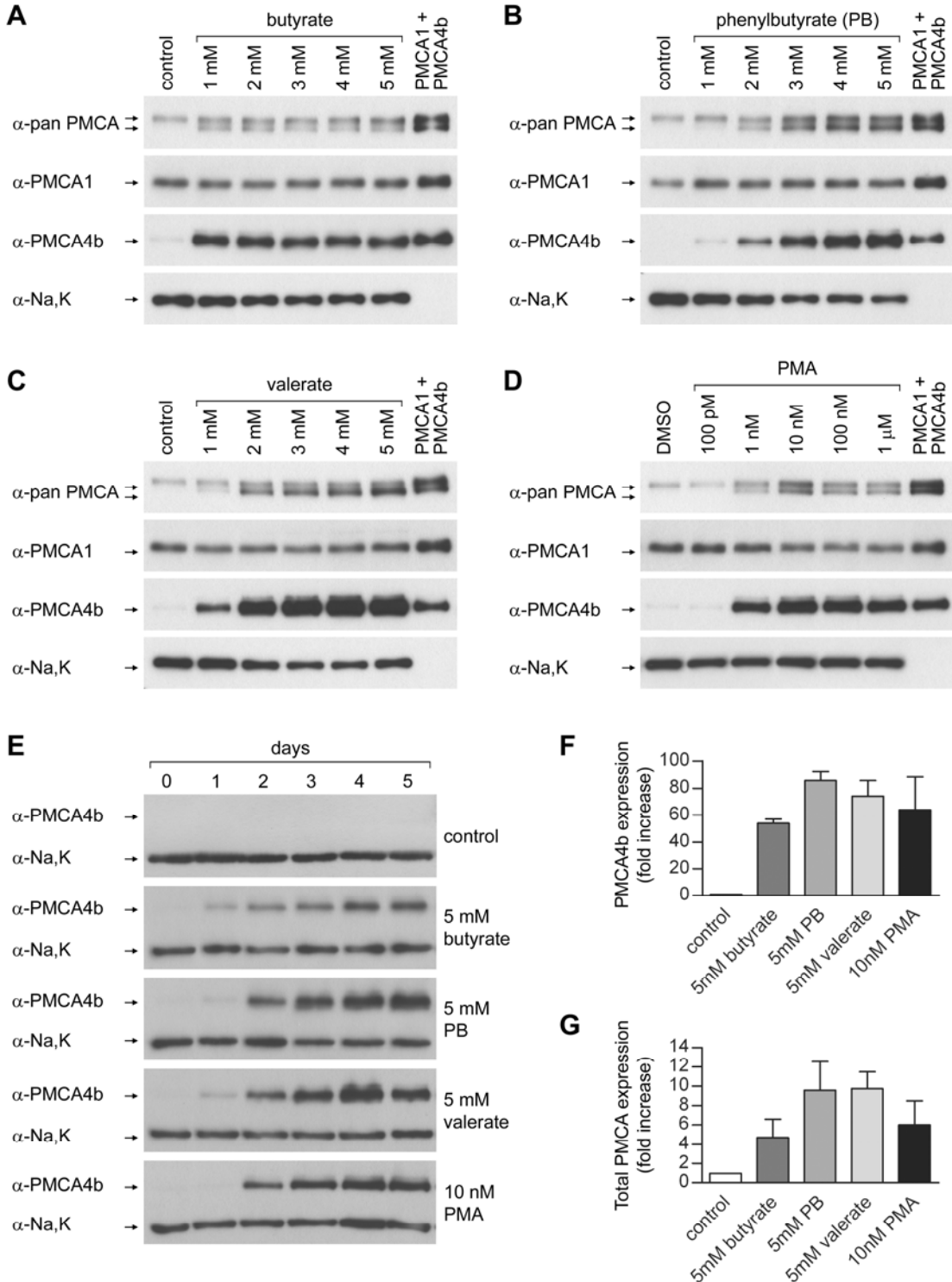


FIGURE 2

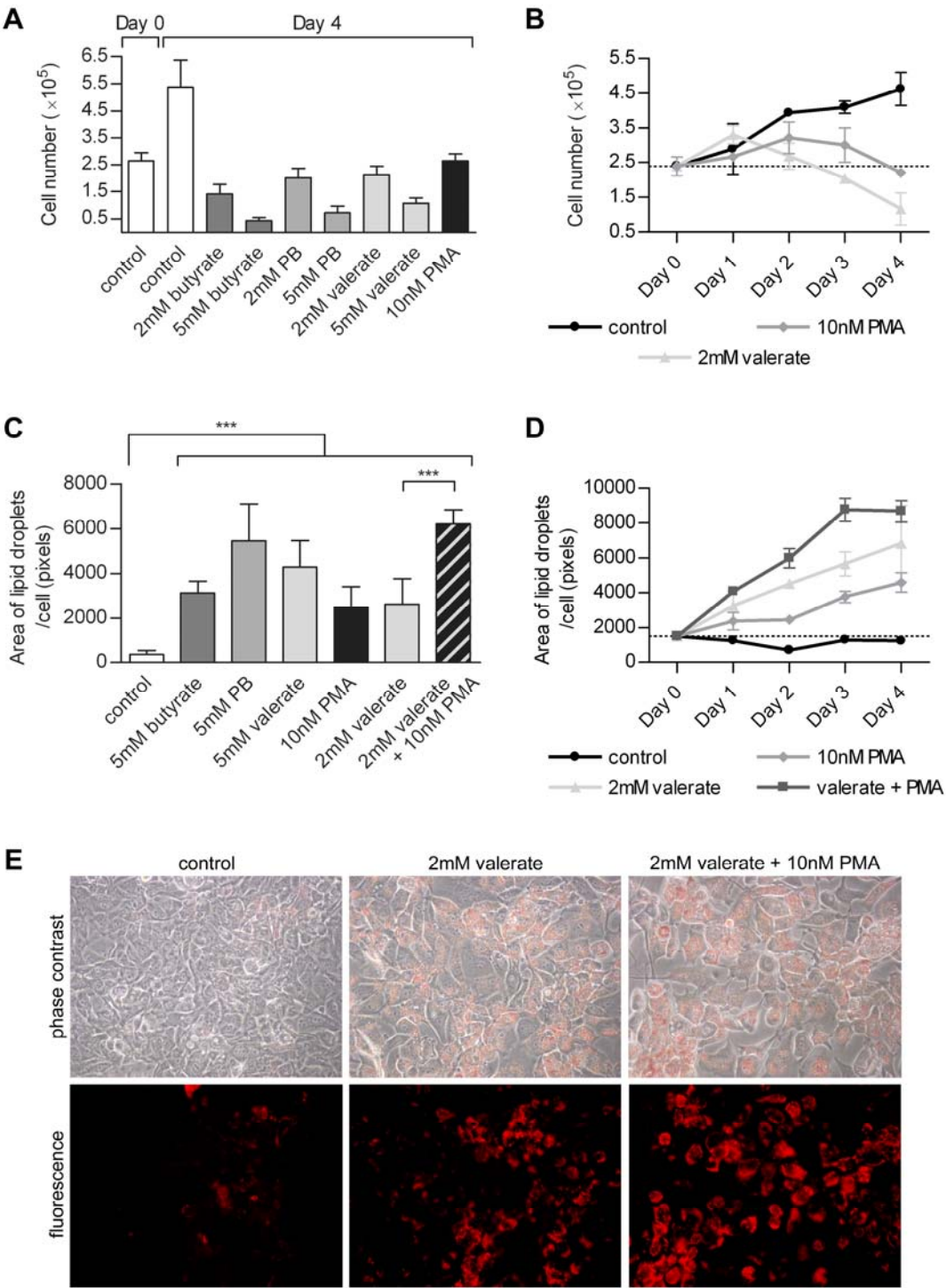


FIGURE 3

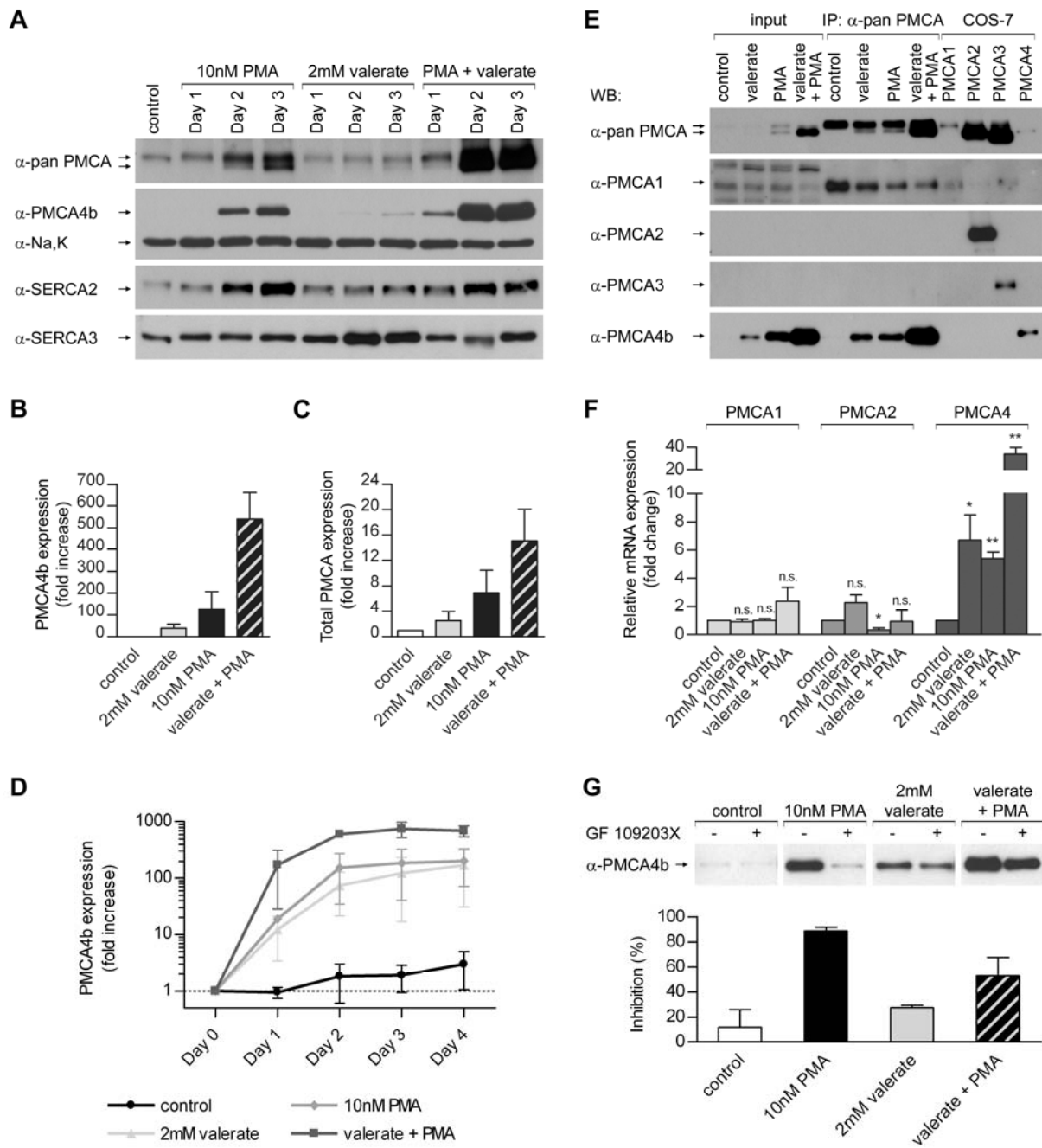


FIGURE 4

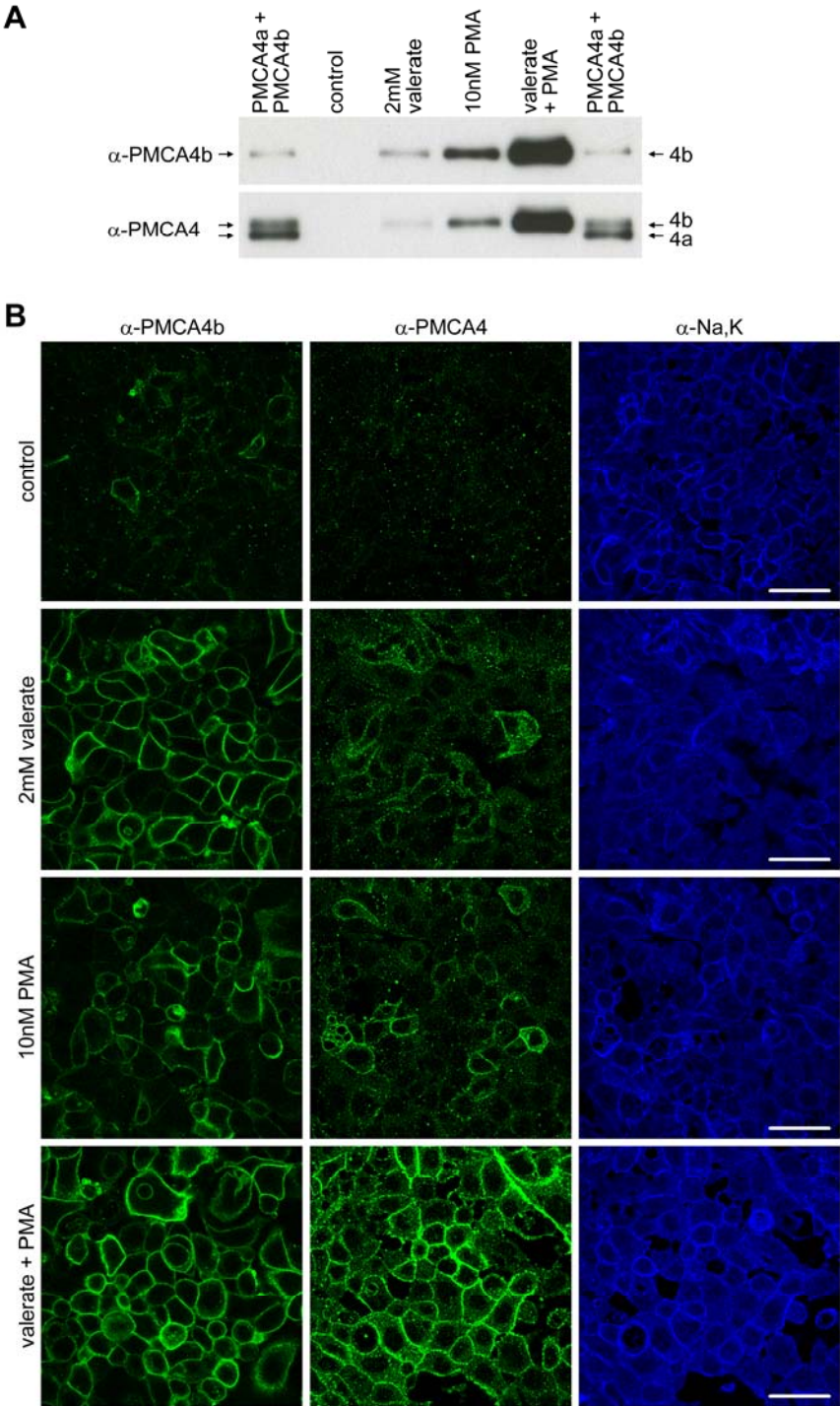


FIGURE 5

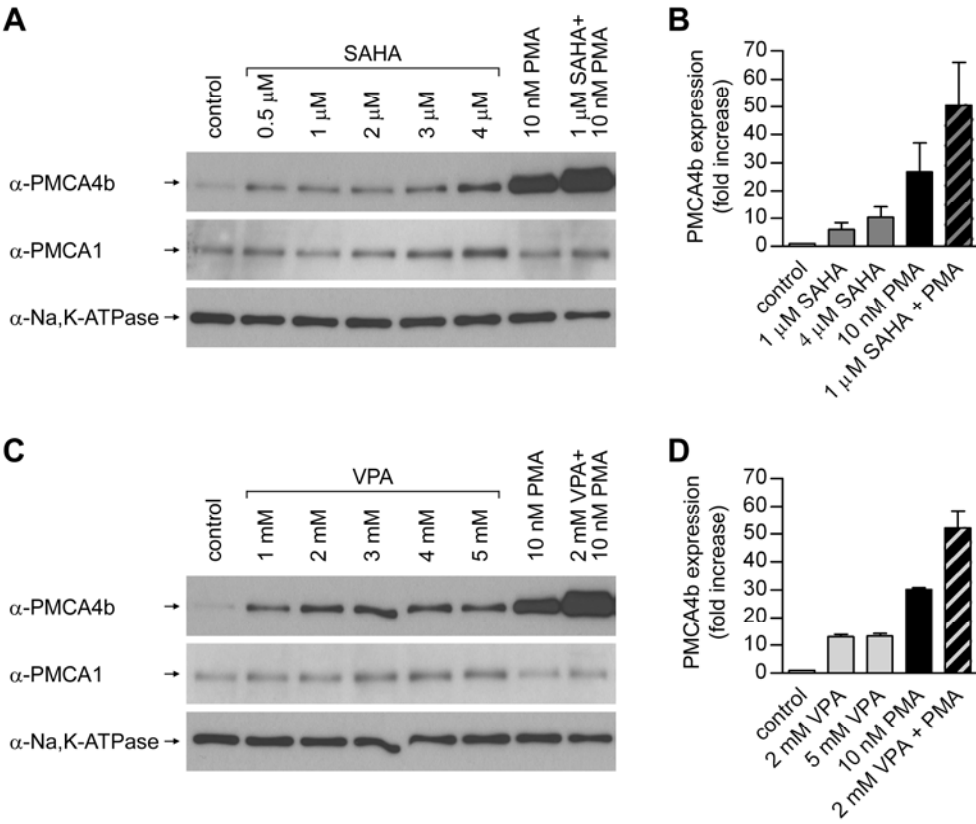


FIGURE 6

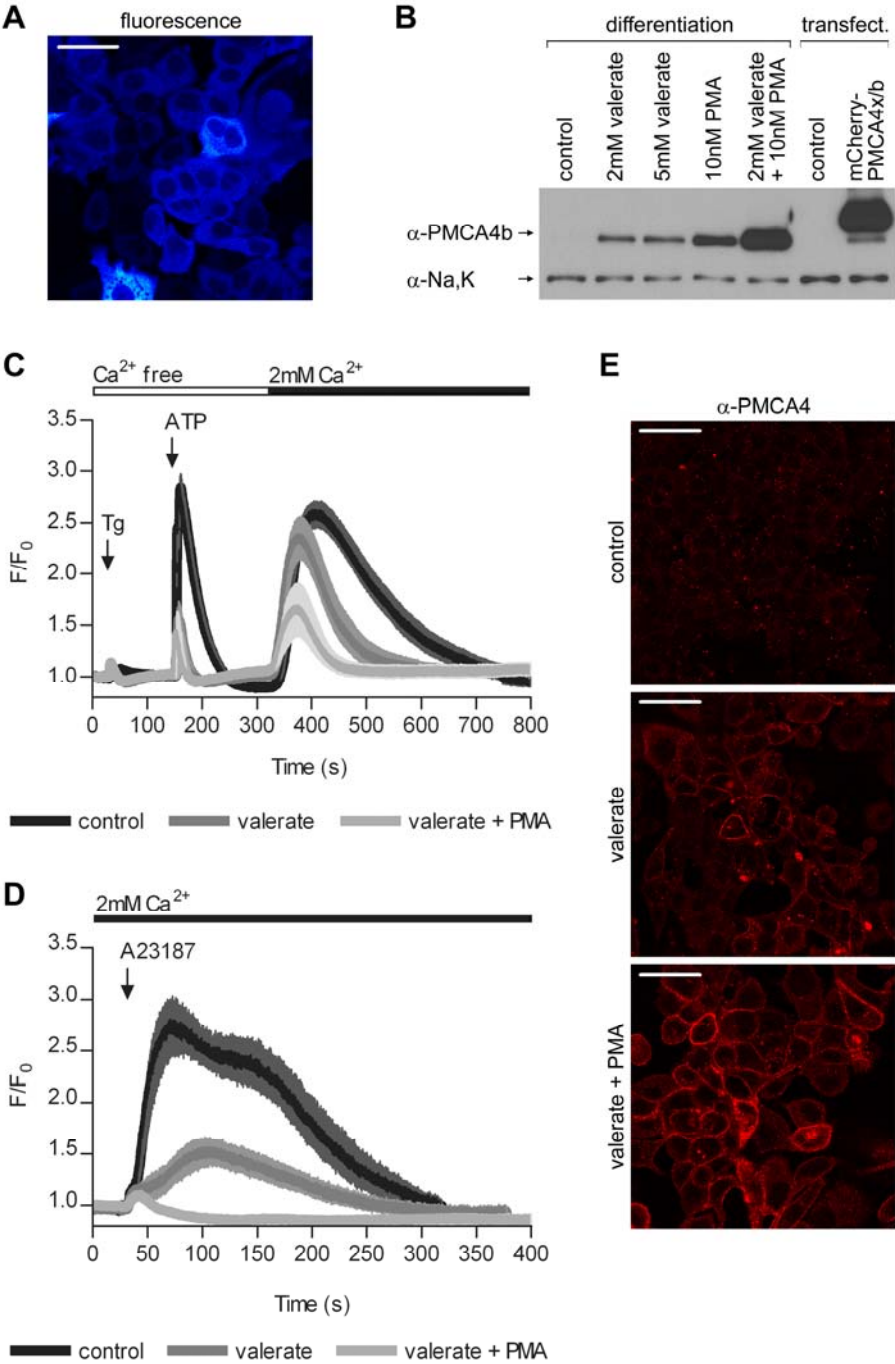


FIGURE 7

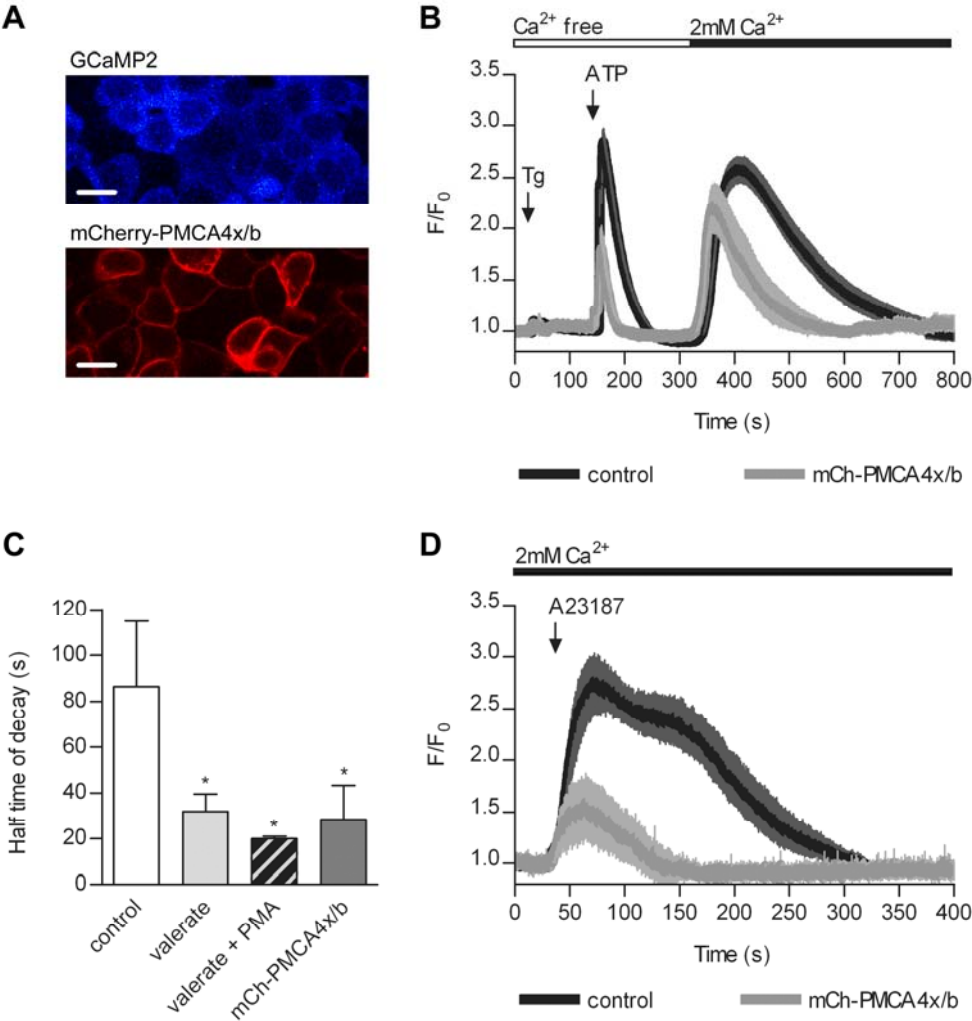


FIGURE 8

